methods; this limitation probably reflects the low solubility of $TaCl_5$.

The possible mechanisms of this ultrasonic activation include (1) the creation of extremely reactive, high dispersions of transition metal on NaCl matrix, (2) improved mass transport between bulk solution and the reactive surfaces, and (3) direct trapping with CO of reactive metallic species formed during the reduction of the metal halide. We can eliminate the first and second mechanism: complete reduction of metal halide by Na with ultrasonic irradiation *under Ar*, followed by exposure to 4.4 atm of CO in the absence or presence of ultrasound, yielded no metal carbonyl. In the case of WCl_6, Fourier transform infrared spectra taken during sonication under CO show the initial formation of tungsten carbonyl halides followed by their conversion to $W(CO)_6$ and finally its further reduction to $W_2(CO)_{10}^{2-}$. Thus the reduction process appears to be sequential, wherein reactive metal species are formed upon partial reduction at the sodium surface and trapped by CO.

These reaction conditions have been run at small scale and may prove uniquely useful, for example, in the production of ^{13}CO labeled carbonyl complexes where the low CO pressures are mandatory. Scale-up of ultrasonic irradiation is, however, extant technology used industrially, e.g., for the production of emulsions.[14] Thus the use of ultrasound in chemical synthesis may well develop an important niche in the chemical community.

Acknowledgment. This research was supported by grants from the National Science Foundation (CHE8319929) and the donors of the Petroleum Research Fund, administered by the American Chemical Society.

Registry No. $W_2(CO)_{10}^{2-}$, 45264-18-4; $Mo_2(CO)_{10}^{2-}$, 45264-14-0; $Cr_2(CO)_{10}^{2-}$, 45264-01-5; $Ta(CO)_6^-$, 45047-35-6; $Nb(CO)_6^-$, 45046-84-2; $V(CO)_6^-$, 20644-87-5; $Mn(CO)_5^-$, 14971-26-7; $Fe(CO)_4^{2-}$, 22321-35-3; $Fe_2(CO)_8^{2-}$, 58281-28-0; $Ni_6(CO)_{12}^{2-}$, 52261-68-4; WCl_6, 13283-01-7; $MoCl_5$, 10241-05-1; $CrCl_3$, 10025-73-7; $TaCl_5$, 7721-01-9; $NbCl_5$, 10026-12-7; VCl_3, 7718-98-1; $VCl_3(THF)_3$, 19559-06-9; CO, 630-08-0; Na, 7440-23-5.

---

[14] (a) Shoh, A. In "Kirk–Othmer Encyclopedia of Chemical Technology", 3rd ed.; Wiley: New York, 1983; Vol. 23, pp 462–479. (b) Cracknell, M. F. *Contemp. Phys.* **1976**, *17*, 13. (c) Murry, E. J. *ChemTech* **1975**, 108, 232, 376.

Distance Dependence of Electron-Transfer Reactions: Rate Maxima and Rapid Rates at Large Reactant Separations

Bruce S. Brunschwig, Stanton Ehrenson, and Norman Sutin*

Department of Chemistry
Brookhaven National Laboratory
Upton, New York 11973

Received August 16, 1984

Early in the history of electron-transfer studies it was pointed out that bimolecular electron transfer can occur over a range of reactant separations.[1] However, the values of certain parameters needed for rate calculations have only recently been determined. Specifically, an increasing amount of experimental data on the distance dependence of the electronic coupling element[2,3] and on the nuclear configuration changes accompanying electron transfer have become available.[4] Important advances in the formulation of the electron-transfer problem have also been made.[5-9] Recently we have undertaken detailed calculations of the distance dependence of the rates of electron-transfer reactions in solution. We find that the dependences of the electronic coupling element and of the solvent reorganization energy on distance have important implications for intramolecular electron transfers and for the forward and back reaction rates and cage-escape yields in light-induced electron-transfer processes.

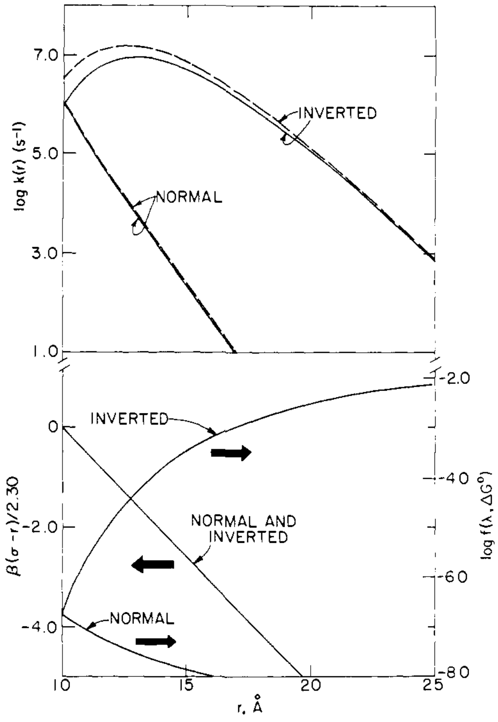

Figure 1. Distance dependence of the first-order rate constant $k(r)$ in the normal and inverted regions, calculated from eq 2–4 using $\beta = 1.2$ Å^{-1}, $H_{AB}° = 200$ cal, $\lambda_{in} = 1.92$ kcal mol^{-1} and $\sigma = 10$ Å. Upper figure: normal region, $\Delta G° = +0.25$ eV; inverted region, $\Delta G° = -2.00$ eV; solid line, classical calculation; dashed line, quantum-mechanical calculation[6] with $\nu_{in} = 450$ cm^{-1}. Lower figure: the distance dependence of the components of $k(r)$; $f(\lambda,\Delta G°) = (1/\lambda^{1/2}) \exp[-(\lambda + \Delta G°)^2/(4\lambda RT)]$.

Since bimolecular electron transfer can occur over a range of separation distances, each with a unique first-order rate constant $k(r)$, the net second-order rate constant for the reaction is given by[1,5]

$$k_{\text{obsd}} = \frac{4\pi N}{1000} \int_0^\infty g(r)k(r)r^2 \, dr \quad M^{-1}\,s^{-1} \qquad (1)$$

where r is the distance between the two redox sites, and $g(r)$ is the pair distribution function. For spherical reactants r is the center-to-center distance and it is generally assumed that $g(r) =$

---

[1] Levich, V. G. *Adv. Electrochem. Electrochem. Eng.* **1966**, *4*, 249. Reynolds, W. L.; Lumry, R. W. "Mechanisms of Electron Transfer"; Ronald Press: New York, 1966.

[2] Miller, J. R.; Beitz, J. V. *J. Chem. Phys.* **1981**, *7*, 6746. Huddleston, R. K.; Miller, J. R. *J. Chem. Phys.* **1982**, *79*, 5337. Miller, J. R.; Hartman, K. W.; Abrash, S. *J. Am. Chem. Soc.* **1982**, *104*, 4296. Miller, J. R.; Peeples, J. A.; Schmitt, M. J.; Closs, G. L. *J. Am. Chem. Soc.* **1982**, *104*, 6488.

[3] Guarr, T.; McGuire, M.; Straugh, S.; McLendon, G. *J. Am. Chem. Soc.* **1983**, *105*, 616. Nocera, D. G.; Winkler, J. R.; Yocum, K. M.; Bordignon, E.; Gray, H. B. *J. Am. Chem. Soc.* **1984**, *106*, 5145. Isied, S. S.; Kuehn, C.; Worosila, G. *J. Am. Chem. Soc.* **1984**, *106*, 1722. McCourty, J. L.; Blough, N. V.; Hoffman, B. M. *J. Am. Chem. Soc.* **1983**, *105*, 4470.

[4] Brunschwig, B. S.; Creutz, C.; Macartney, D. H.; Sham, T. K.; Sutin, N. *Faraday Discuss. Chem. Soc.* **1982**, *74*, 113. Szalda, D. J.; Creutz, C.; Mahajan, D.; Sutin, N. *Inorg. Chem.* **1983**, *22*, 2372. Szalda, D. J.; Macartney, D. H.; Sutin, N. *Inorg. Chem.* **1984**, *23*, 3473.

[5] (a) Marcus, R. A *Int. J. Chem. Kinet.* **1981**, *13*, 865. (b) Marcus, R. A.; Siders, P. *J. Phys. Chem.* **1982**, *86*, 622. (c) Siders, P.; Marcus, R. A. *J. Am. Chem. Soc.* **1981**, *103*, 741. (d) Marcus, R. A. *Faraday Discuss. Chem. Soc.* **1982**, *74*, 7.

[6] Kestner, N. R.; Logan, J.; Jortner, J. *J. Phys. Chem.* **1974**, *78*, 2148. Brunschwig, B. S.; Logan, J.; Newton, M. D.; Sutin, N. *J. Am. Chem. Soc.* **1980**, *102*, 5798. Bixon, M.; Jortner, J. *Faraday Discuss. Chem. Soc.* **1982**, *74*, 17.

[7] Newton, M. D. *ACS Symp. Ser.* **1982**, *No. 198*, 255. Tembe, L.; Friedman, H. L.; Newton, M. D. *J. Chem. Phys.* **1982**, *76*, 1490. Friedman, H. L.; Newton, M. D. *Faraday Discuss. Chem. Soc.* **1982**, *74*, 73.

[8] For recent reviews, see: Sutin, N. *Prog. Inorg. Chem.* **1983**, *30*, 441. Newton, M. D.; Sutin, N. *Annu. Rev. Phys. Chem.* **1984**, *35*, 437.

[9] Sutin, N.; Brunschwig, B. S. *ACS Symp. Ser.* **1982**, *No. 198*, 105. Sutin, N. *Acc. Chem. Res.* **1982**, *15*, 275.

0002-7863/84/1506-6858$01.50/0

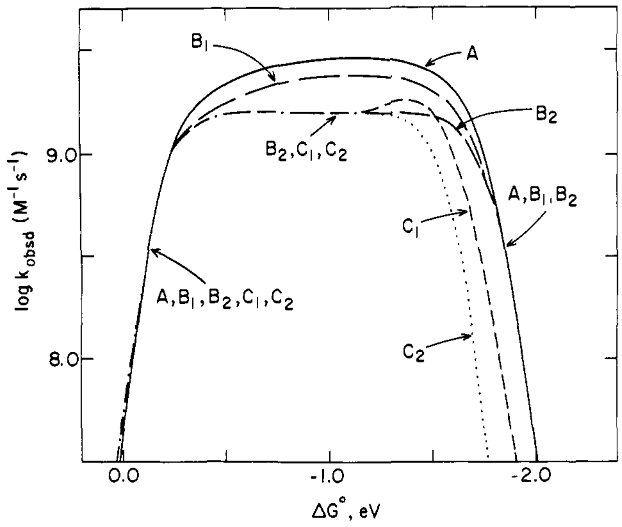

Figure 2. Plot of the logarithm of the second-order rate constant vs. driving force for reactants with charges +2 and +3, 0.5 M ionic strength, with $D = 3 \times 10^{-6}$ cm^2 s^{-1} and the parameters in the caption to Figure 1. A, solid curve, eq 1 with a steady-state solution to the diffusion equation;[5b] B_1, long dashes, eq 5 combined with eq 6 and 7, but with lower limit of integration equal to the separation distance that maximizes k_{obsd}; B_2, long dashes, as for B_1 except that lower limit of integration is equal to σ; C_1, short dashes, eq 5 with k_{diff} given by eq 6 but with lower limit of integration equal to r_m, the separation distance corresponding to the maximum value of k_{act}, and k_{act} given by the eq 8 with δr equal to $1/\beta$; C_2, dotted curve, as for C_1 but with r_m equal to σ.

0 for $r < \sigma$, where σ is the sum of the hard-sphere radii of the two reactants.[10] The value of $g(r)$ can be obtained by solving a diffusion equation in which the gradients due to diffusion, conduction, and reaction are considered.[5b] For a reaction that is marginally nonadiabatic ($H_{AB} \lesssim 200$ cal) at close contact of the reactants, $k(r)$ is given by[5-9]

$$k(r) = \frac{2H_{AB}^2}{h}\left[\frac{\pi^3}{\lambda RT}\right]^{1/2} \exp\left[-\frac{(\lambda + \Delta G^\circ)^2}{4\lambda RT}\right] \text{ s}^{-1} \quad (2)$$

$$H_{AB}^2 = (H_{AB}^\circ)^2 \exp[-\beta(r - \sigma)] \quad (3)$$

where ΔG° is the driving force for the reaction and H_{AB} is the electronic coupling element. The (vertical) reorganization energy λ contains inner-shell (λ_{in}) and solvent (λ_{out}) contributions: λ_{in} is independent of r, while λ_{out} is given in the conducting-sphere approximation by[11]

$$\lambda_{out} = (\Delta e)^2\left[\frac{1}{2a_1} + \frac{1}{2a_2} - \frac{1}{r}\right]\left[\frac{1}{D_{op}} - \frac{1}{D_s}\right] \quad (4)$$

where a_1 and a_2 are the hard-sphere radii of the two reactants and D_{op} and D_s are the optical and static dielectric constants of the solvent.

In Figure 1 we show the dependence of $k(r)$ on r calculated from eq 2–4 for $\Delta G^\circ = +0.25$ eV (normal region) and -2.0 eV (inverted region), using $\beta = 1.2$ Å^{-1}, $H_{AB}^\circ = 200$ cal, $\lambda_{in} = 1.92$ kcal mol^{-1}, and $\sigma = 10$ Å. In the normal region the maximum value of $k(r)$ is at close contact, as expected. In the inverted region the rates at large separation are several orders of magnitude larger than those in the normal region and $k(r)$ has a maximum at $r > \sigma$. As is illustrated in the lower part of the figure, the rate maximum is a consequence of the opposing effects of separation distance on $|H_{AB}|$ (eq 3) and λ_{out} (eq 4). The nuclear tunneling corrections[6] (dashed lines, upper part of figure) are never very large[12] and become negligible at large separations.

Bimolecular rate constants calculated with different expressions for k_{obsd} are compared in Figure 2.[13] The largest rate constants are obtained from eq 1 with $g(r)$ obtained from the steady-state solution to the diffusion equation (A, solid line). Under steady-state conditions k_{obsd} can also be calculated from eq 5–7,[5] where

$$1/k_{obsd} = (1/k_{diff}) + (1/k_{act}) \quad (5)$$

$$k_{diff} = \frac{4\pi ND}{1000} \Big/ \int_\sigma^\infty (g_e(r)r^2)^{-1}\,dr \quad (6)$$

$$k_{act} = \frac{4\pi N}{1000}\int_\sigma^\infty g_e(r)k(r)r^2\,dr \quad (7)$$

k_{diff} is the diffusion-controlled rate constant, k_{act} is the activation-controlled rate constant, D is the sum of the diffusion coefficients of the two reactants, and $g_e(r)$ is the *equilibrium* pair distribution function equal to $\exp(-U(r)/RT)$ where $U(r)$ is the interaction energy of the reactants. (A Debye–Hückel potential is usually used for $U(r)$.) It is apparent from Figure 2 that the rates in the diffusion-controlled region calculated from eq 5–7 (B_2, long dashes) are significantly lower than those calculated from the more rigorous eq 1. Also shown (B_1, long dashes) is the effect of increasing the lower limit of integration in eq 6 and 7 so as to maximize k_{obsd}: as expected, this causes the diffusion-controlled rate to increase with driving force. In another approximation[9] the integral in eq 7 is replaced by the maximum value of the integrand to yield eq 8 where $r_m \geq \sigma$ and $\delta r = 1/\beta$. Rates

$$k_{act} = \frac{4\pi N r_m^2}{1000} g_e(r_m)k(r_m)\,\delta r \quad (8)$$

calculated with eq 8 and k_{diff} integrated from r_m (C_1, short dashes) are lower in the inverted region primarily as a result of the use of a driving-force-independent δr. Finally, even lower rates (C_2, dotted curve) are calculated by using eq 8 when the traditional assumption that $r_m = \sigma$ is introduced for both k_{act} and k_{diff}.

The above analysis shows that reactions at moderate driving force (i.e., in the normal region) can have rate maxima at close contact of the reactants while reactions with large driving force (i.e., in the inverted region) have rate maxima at larger separations. This has the following consequences: (1) For a system in the inverted region a maximum in the rate for *intramolecular* electron transfer should be observed as a function of separation distance when the length of the bridging group is systematically increased from the close-contact distance at constant driving force. (2) In *bimolecular* reactions that are photoinduced, the forward (quenching) reaction is usually in the normal region while the back reaction (to form ground-state reactants) often lies in the inverted region.[14] Consequently the maximum rate for the forward reaction will generally occur at shorter distances ($r_m \sim \sigma$) than the maximum rate of the back reaction ($r_m > \sigma$).[15] In other words, the rate constant for the back reaction will initially increase as the primary products diffuse out of the reaction cage in which they were formed. This difference in the optimum distance for the forward and back reactions has important implications for the formulation of steady-state quenching schemes and for the interpretation of cage-escape yields.[16]

Acknowledgment. We thank Dr. C. Creutz for helpful discussions. This research was carried out at Brookhaven National Laboratory under Contract DE-AC02-76CH00016 with the U.S. Department of Energy and supported by its Division of Chemical Sciences, Office of Basic Energy Sciences.

---

(10) Interpenetration of the inner coordination shells of the two reactants is considered in ref. 7.

(11) Marcus, R. A. *J. Chem. Phys.* **1956**, *24*, 966.

(12) The nuclear-tunneling corrections will, however, be larger if a (high-frequency) intraligand mode (1300 cm^{-1})[5b] rather than a metal–ligand stretching mode (450 cm^{-1}) is relevant to λ_{in}.

(13) Bimolecular reaction at large separations is favored by the r^2 (shell volume) factor and, for similarly charged reactants, also by $g(r)$, in addition to the factors considered for intramolecular reactions.

(14) Sutin, N.; Creutz, C. *J. Chem. Educ.* **1983**, *60*, 809.

(15) The possibility of different distance dependences of the electronic coupling elements for the forward and back reactions has been considered by: Mauzerall, D.; Ballard, S. G. *Annu. Rev. Phys. Chem.* **1982**, *33*, 377.

(16) Although the above results were derived for a specific model, their generality is being examined with alternative models for λ_{out} and for the distance dependence of H_{AB}.